Characterization of GRIIRA properties in LiNbO3 and LiTaO3 with different compositions and doping

Article *in* Proceedings of SPIE - The International Society for Optical Engineering · March 2008

DOI: 10.1117/12.773742

5 authors, including:

Junji Hirohashi
OXIDE corporation
56 PUBLICATIONS **360** CITATIONS
SEE PROFILE

Akiya Miyamoto
High Energy Accelerator Research Organization
406 PUBLICATIONS **8,361** CITATIONS
SEE PROFILE

Characterization of GRIIRA properties in $LiNbO_3$ and $LiTaO_3$ with different compositions and doping

J. Hirohashi, T. Tago, O. Nakamura, A. Miyamoto, and Y. Furukawa
Oxide Corp., 1747-1 Mukawa, Hokuto Yamanashi, 408-0302 JAPAN

ABSTRACT

Green-induced infrared absorption (GRIIRA) properties were characterized for $LiNbO_3$ (LN) and $LiTaO_3$ (LT) single crystals. GRIIRA was measured using a photothermal common-path interferometer. Several LN and LT with different concentrations and doping materials were investigated. Mg-doped near-stoichiometric LT (Mg-SLT) had the lowest IR absorption. In addition, no GRIIRA was observed only in MgSLT. Therefore, Mg-SLT could be the most suitable material for high power green generation. In LN crystals, higher GRIIRA was observed in non-doped congruent LN (CLN) which has low photorefractive damage threshold. The 1.3 mol% Mg doped SLN had the lowest GRIIRA within the investigated LN crystals. Even in the materials with low GRIIRA, two different characteristics were observed; initially high IR absorption and slow relaxation time of GRIIRA. The first characteristic was observed for Mg doped LN which has a higher number of scattering centers. The second was strongly observed in Mg doped LN which has a higher level of absorption in the UV region.

Keywords: $LiNbO_3$, $LiTaO_3$, stoichiometry, green light induced-absorption

1. INTRODUCTION

Nonlinear optical frequency conversion is one of the most important key techniques to obtain lasers with wavelengths targeted for specific applications. In order to realize efficient and tailored lasers, the quasi-phase-matching (QPM) approach using periodically-poled ferroelectric crystals is becoming important. In particular, by developing the periodic-poling technique, applications of these devices in visible light and high power generation have become more attractive.

To realize these applications, there are several important optical properties; high nonlinearity and low absorption. From the point of nonlinearity, the most attractive material group is $LiNbO_3$ and $LiTaO_3$. For example, the nonlinear coefficient d_{33} of $LiNbO_3$ is approximately 1.7 times larger than that of $KTiOPO_4$ crystal.[1] In addition, since they are grown by Czochralski growth method, it is possible to grow larger size crystals, hence, they may be produced more cheaply than other nonlinear materials.

Material absorption is also important especially in applications for high-power visible second-harmonic generation. In addition, it is impossible to neglect visible light induced absorption such as green-light induced infrared absorption (GRIIRA). These properties are very critical for designing laser cavities.

In our group, so far, we have been exploring material solutions for these applications. In particular, we have been continuously developing our crystal growth technique to realize $LiNbO_3$ and $LiTaO_3$ with high nonlinearity and low absorption. In order to do these developments, it is important not only to optimize the growth process but also to characterize their optical properties. In this work, we report GRIIRA properties of several $LiNbO_3$ and $LiTaO_3$ crystals with different doping and different Li concentrations by using photo-thermal common path interferometer technique.

2. SAMPLE PREPARATION

Several different crystals were grown by conventional Czchoralski growth and novel double-crucible Czchoralski growth technique. Investigated materials are listed in Table I. Non-doped conventional congruent $LiNbO_3$ was investigated as a

Nonlinear Frequency Generation and Conversion: Materials, Devices, and Applications VII, edited by Peter E. Powers,
Proc. of SPIE Vol. 6875, 687516, (2008) · 0277-786X/08/$18 · doi: 10.1117/12.773742

reference. Mg, Sc, and Mg-Ge were selected as doping materials to compensate for the photorefractive damage. Li concentration was also changed to investigate the effect of stoichiometry.

After growing the crystals, we poled them to make them single domain crystals. The samples with 5-mm in Z direction are prepared and polished in Y and Z surfaces. Photorefractive damage properties are confirmed by irradiating 532 nm CW green light with 300 mW into a spot size of 70 μm in diameter. No remarkable photorefractive damage was observed except for in the non-doped congruent $LiNbO_3$ sample.

Table 1. Investigated materials

Sample number	Crystal	Li concentration	Doping material	Doping concentration	Abbreviation
A	$LiTaO_3$	near-stoichiometric	Mg	1.0 mol%	Mg-SLT
B	$LiNbO_3$	congruent	None	None	CLN
C	$LiNbO_3$	congruent	Mg	5.0 mol%	Mg-CLN
D	$LiNbO_3$	congruent	Mg Ge	5.0 mol% 1.0 mol%	MgGe-CLN
E	$LiNbO_3$	near-stoichiometric	Sc	0.4 mol%	Sc-SLN
F	$LiNbO_3$	near-stoichiometric	Mg	1.8 mol%	1.8 Mg-SLN
G	$LiNbO_3$	near-stoichiometric	Mg	1.3 mol%	Mg-SLN
H	$LiNbO_3$	near-stoichiometric	Mg	1.3 mol%	Mg-SLN

3. EXPERIMENTAL SETUP

A schematic of the experimental set-up is shown in Fig. 1. Photo-thermal common path interferometer system (PCI-3, Stanford Photo-thermal Solution) was used in this study. [2-5] Three laser beams were aligned through the sample: a probe beam at 633 nm (He-Ne) with 200 μm in diameter, a continuous wave pump beam of IR (1064 nm: Light wave model 221) with 70 μm in diameter, and a continuous wave 2nd pump beam of green (532 nm: Melles Griot diode pumped solid state laser) with 70 μm in diameter. The IR pump beam was mechanically chopped at an arbitrary frequency (in this study, 420 kHz), which produced periodic heating of the sample by pump beam. The probe beam senses the heating effect of the absorbed pump. Smalls modulation of the probe signals were picked up by the photodetector and processed by a lock-in amplifier that is tuned to the chopping frequency.

The IR pump power was set to 1 W after chopping. That is, an IR peak intensity at the focused position corresponds to approximately 50 kW/cm^2. Three different green pump power conditions (0.1 W, 1.0 W, and 1.9 W) were tested. The polarization of the three beams was fixed in the crystallographic y-axis for all experiments.

By using this system, it is possible to characterize sample absorption signals for the pump beam. The measured signals are calibrated by the glass sample (Schott NG12 ND filter). As a result, it is possible to calculate absolute value of the absorption coefficient of the sample..

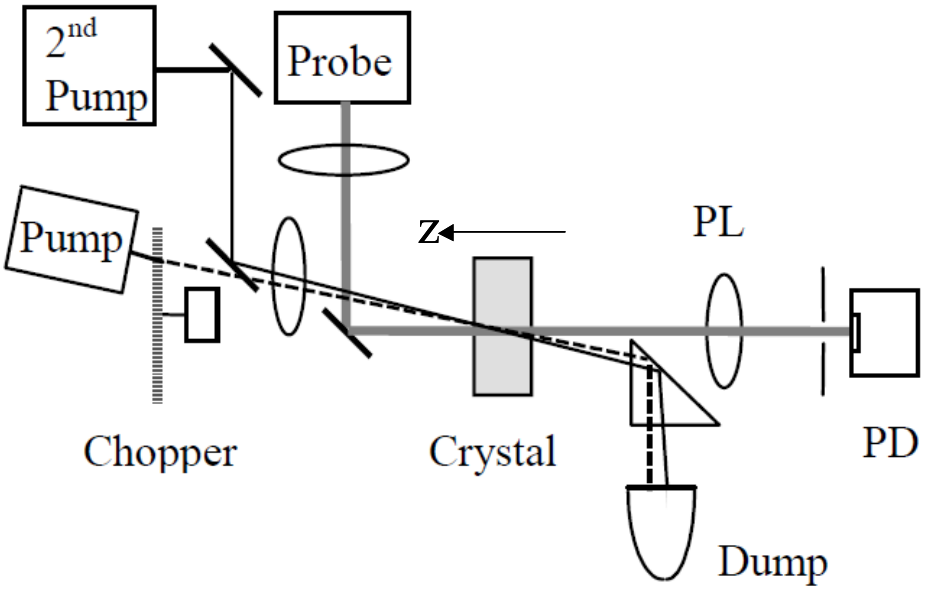

Fig. 1. Schematic of experimental set up of photo-thermal common path interferometer.[2]

PL: projection lens, PD: photodiode

By scanning the sample in the z-direction in Fig. 1, it is possible to measure the bulk and surface absorption of the sample. Typical scanned absorption signal of $LiNbO_3$ is shown in Fig. 2. In Fig. 2, the position at z = 1.8 and 2.8 mm could be the signal of both bulk and surface absorption. Therefore, the signal between these two peaks (around z = 2.2 mm position in the Fig. 2) was chosen as a bulk signal in the following results.

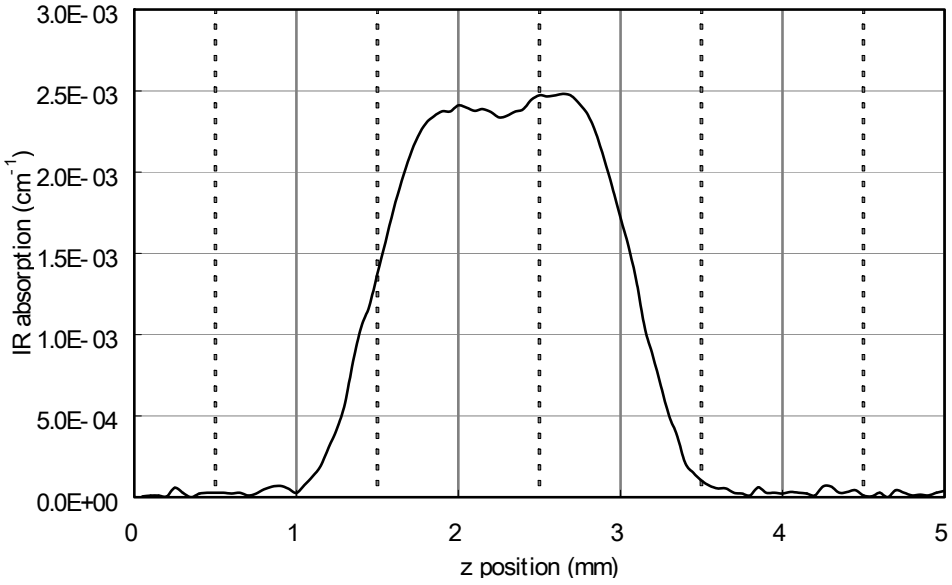

Fig. 2. Typical IR absorption profile

4. RESULT AND DISCUSSION

Table 2 shows measured IR absorption of the investigated materials. The smallest absorption is for the Mg-SLT. Considering $LiNbO_3$, the congruent $LiNbO_3$ (samples B, C, and D) has 2 to 8 times higher absorption than the stoichiometric $LiNbO_3$ (samples E, G, and H). This could indicate that Li vacancies create absorption centers and as a result, fewer Li vacancies might be better to reduce the IR absorption. Here it is important to note that sample F (1.8 Mg-SLN) shows one order higher absorption than sample G and H (Mg-SLN). Since sample F has higher number of scattering centers than sample G and H, the IR absorption might increase even though the Li composition is near stoichiometric. Therefore, it is important not only to control the stoichiometric concentration but also to reduce macroscopic defects.

Table 2. Measured IR absorption for each sample

Sample number	Crystal	IR absorption (cm^{-1})
A	Mg-SLT	0.2×10^{-3}
B	CLN	2.4×10^{-3}
C	Mg-CLN	2.6×10^{-3}
D	MgGe-CLN	1.8×10^{-3}
E	Sc-SLN	0.8×10^{-3}
F	1.8 Mg-SLN	9.8×10^{-3}
G	Mg-SLN	0.3×10^{-3}
H	Mg-SLN	0.4×10^{-3}

Next, GRIIRA properties are investigated. Typical GRIIRA profiles of $LiNbO_3$ and $LiTaO_3$ are shown in Fig. 3. In this study, GRIIRA value was defined as the difference between initial IR absorption and IR absorption under green light irradiation as shown in Fig. 3. In all cases, green light was irradiated for 40 to 50 s.

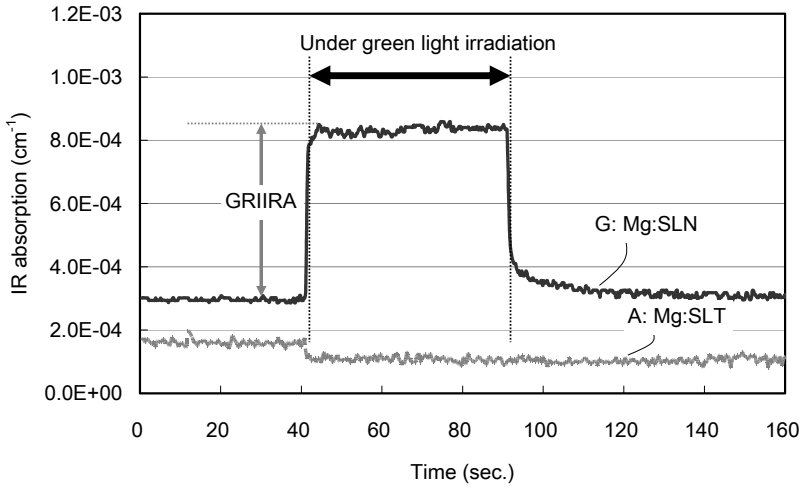

Fig. 3. Typical measured GRIIRA profiles of $LiNbO_3$ and $LiTaO_3$

As shown in Fig. 3, no GRIIRA was observed only in the case of Mg-SLT (sample A). Small decrease of IR absorption after irradiation of green light occurred only one time (the first irradiation of green light). Similar tendency was also observed in Ref. 2. From this result, Mg-SLT has better GRIIRA properties than other $LiNbO_3$.

On the contrary, all $LiNbO_3$ show GRIIRA in the present experimental condition. Figure 4 shows dependency of GRIIRA on green intensity for investigated $LiNbO_3$. As shown in Fig. 4(a), non-doped CLN (sample B) has stronger GRIIRA than other doped $LiNbO_3$. It has also higher dependency of GRIIRA on the irradiated green intensity. One reason for this high dependency would be the photorefractive effect. For doped-$LiNbO_3$ (samples C, D, E, and H), there is a slight dependence of GRIIRA on the intensity of green light. The dependency is slightly different from sample to sample, but there was no obvious correlation between this tendency and doping materials or Li concentrations. Further investigation is needed in the future to explain these small differences.

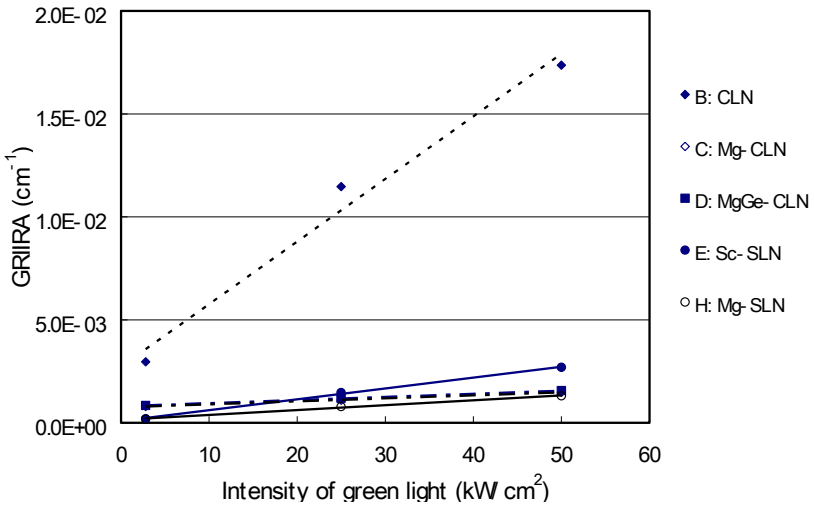

(a)

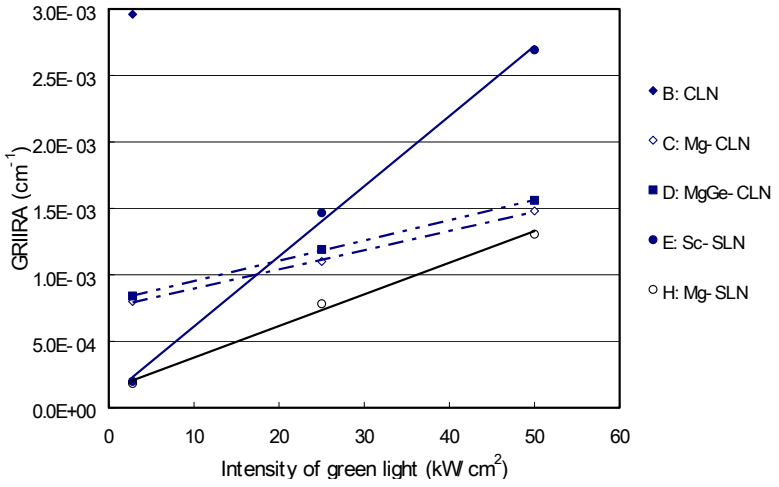

(b)

Fig. 4. Dependency of GRIIRA on green intensity

(a): comparison between CLN and doped LN. (b): comparison among doped LN

In Table 3, measured GRIIRA under irradiation of 25 kW/cm^2 green light is summarized. In here, 1.3 mol% Mg-SLN (samples G and H) give the best GRIIRA properties in $LiNbO_3$ again. It is important to note that, in the case of sample F, GRIIRA was not too high even though the IR absorption is one order larger. That might indicate that GRIIRA is not strongly related to the IR absorption itself.

Table 3. GRIIRA under irradiation of 25kW/cm^2 green light

Sample number	Crystal	GRIIRA (cm^{-1})
A	Mg-SLT	None
B	CLN	11.5 X 10^{-3}
C	Mg-CLN	1.1 X 10^{-3}
D	MgGe-CLN	1.2 X 10^{-3}
E	Sc-SLN	1.5 X 10^{-3}
F	1.8 Mg-SLN	1.5 X 10^{-3}
G	Mg-SLN	0.6 X 10^{-3}
H	Mg-SLN	0.8 X 10^{-3}

Finally, GRIIRA decay properties are discussed. Figure 5 shows two different types of GRIIRA decay profiles for Mg-SLN (samples G and H). Irradiated green power was 25 kW/cm^2 and duration time was 50 s. In the case of sample G, IR absorption quickly returned to the original values (within a few seconds) after green light irradiation was stopped. On the contrary, in the case of sample H, IR absorption decreased slowly and it took more than a minute to return to the original IR absorption value. This slow decay might be related to the life time of the trapping sites. That means there might be different types of trapping level in sample H. These trapping levels would be caused by some impurity ions in the samples.

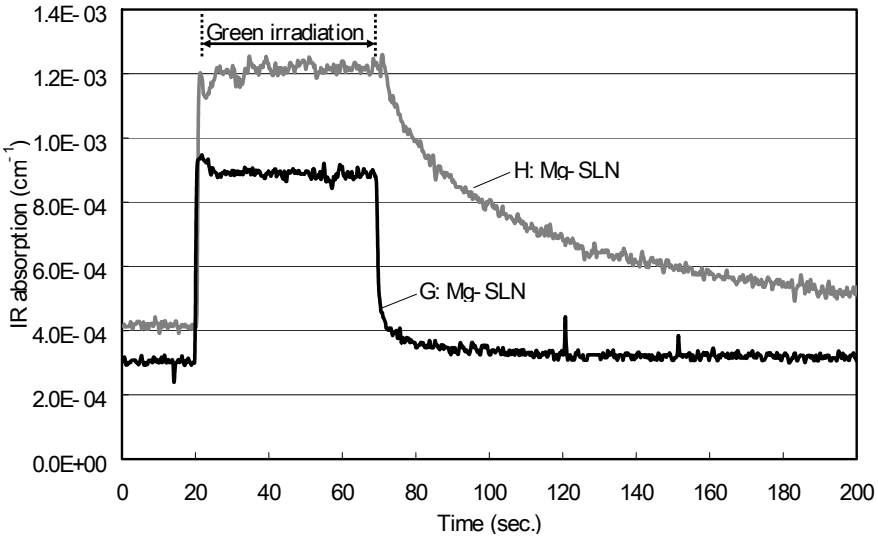

Fig. 5. GRIIRA decay profiles of 1.3 mol% Mg-SLN (sample G and H)

To investigate this difference in detail, transmission curves of the two samples were measured using a spectrophotometer (Hitachi U-4100). Figure 6 shows the measured results for the 5 mm length sample. The transmission at more than 400 nm is almost the same in both samples; however, sample H has a quite high absorption at around UV range (300 to 400 nm) compared to sample G. This result indicates that sample H has additional absorption centers compared with sample G. These absorption centers do not affect the GRIIRA amount itself, but once the electrons or holes are trapped by these additional centers, these trapped ones might relax slowly. As a result, the decay time of GRIIRA would be slow in sample H.

The origin of these additional absorption centers have not yet been clearly found, but they might come from the ion contamination during the crystal growth process.

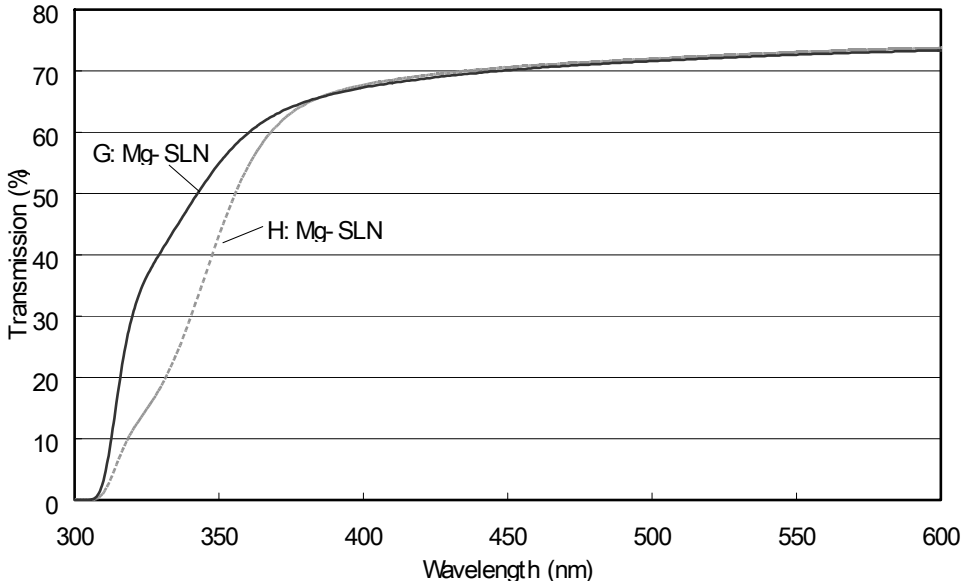

Fig. 6. Transmission curves of 1.3 mol% Mg-SLN (sample G and H)

5. SUMMARY

Green-induced infrared absorption (GRIIRA) properties were characterized for $LiNbO_3$ (LN) and $LiTaO_3$ (LT) single crystals. GRIIRA was measured using a photothermal common-path interferometer. The intensity of the inducing CW-green light was changed from 3 to 50 kW/cm^2. Several LN and LT with different concentrations (from congruent to near-stoichiometric) and doping materials (Mg, Ge, and Sc) were investigated. Mg-doped near-stoichiometric LT (Mg-SLT) had the lowest IR absorption of all the measured samples. In addition, no GRIIRA was observed only in Mg-SLT. Hence, Mg-SLT could be the most suitable material for high power green generation. In LN crystals, IR absorption of near-stoichiometric LN (SLN) was generally lower than that of congruent LN (CLN) in any doping materials. Higher GRIIRA was observed in non-doped CLN, which has low photorefractive damage threshold. 1.3 mol% Mg doped SLN had the lowest GRIIRA within the investigated LN crystals. Even in the materials with low GRIIRA, two different characteristics were observed; initially high IR absorption and slow relaxation time of GRIIRA. The first characteristic was observed for Mg doped LN which has a higher number of scattering centers. The second one was strongly observed in Mg doped LN which has a higher level of absorption in the UV region. We continue to explore new material solutions with better optical qualities by developing crystal growth and post-growth techniques.

REFERENCES

[1] I. Shoji, T. Kondo, A. Kitamoto, M. Shirane, and R. Ito, J. Opt. Soc. Am. B, **14**, 2268 (1997).
[2] A. L. Alexandrovski, G. Foulon, L. E. Myers, R. K. Route, and M. M. Fejer, Proc. SPIE **3610**, 44 (1999).
[3] S. Wang, V. Pasiskevicius, and F. Laurell, J. Appl. Phys. **96**, 2023 (2004).
[4] A. Marcano, O. C. Loper, and N. Melikechi, Appl. Phys. Lett., **78**, 3415 (2001).
[5] M. Roth, N. Angert, M. Tseitlin, and A. Alexandrovski, Optical Mater., **16**, 131 (2001).